Chapter

Highway PC Bridge Inspection by 3.95 MeV X-Ray/Neutron Source

Mitsuru Uesaka, Katsuhiro Dobashi, Yuki Mitsuya, Jian Yang and Joichi Kusano

Abstract

We have developed portable 950 keV/3.95 MeV X-ray/neutron sources and applied them to inspection of PC concrete thicker than 200 mm within reasonable measuring time of seconds - minutes. T-girder-, Box- and slab- bridges are considered. Now we are to start X-ray transmission inspection for highway PC bridge (box) by using 3.95 MeV X-ray sources in Japan in 2020. By obtaining X-ray transmission images of no-grout-filling in PC sheath and thinning of PC wires, we plan to carry out numerical structural analysis to evaluate the degradation of strength. Finally, we are going to propose a technical guideline of nondestructive evaluation (NDE) of PC bridges by taking account of both X-ray inspection and structural analysis. Further, we are trying to detect rainwater detection in PC sheath, and asphalt and floor slab by the 3.95 MeV neutron source. This is expected to be an early degradation inspection. We have done preliminary experiments on X-ray transmission imaging of PC wires and on-grout-filling in the same height PCs in 450–750 mm thick concretes. Moreover, neutron back scattering detection of water in PC sheath is also explained.

Keywords: on-site bridge inspection, highway PC bridge, 950 keV/3.95 MeV X-ray sources, 3.95 MeV neutron source, non-grout-filling, PC wires thinning, rain-water-detection, structural analysis, guideline of nondestructive evaluation

1. Introduction

Since PC (Pre-stressed) bridges were first constructed, about 40 years has passed. Then, the degradation and problems such as no-grout-filling, rail-water-invasion, corruption, thinning and disconnection of PC bridges has revealed and been detected. In these tens years, several nondestructive and destructive evaluations have been performed. Depending on the seriousness of degradation, a few PC bridges are under reconstruction and its planning. So far, they have mainly used inspection by eyes and hammering. However, it is very hard to evaluate the problems and degradation of PC by the above methods. There are non-destructive methods to check PC such as ultrasonography, radar, X-ray transmission by X-ray tubes (200–400 kV), magnetic field detection, etc. But, practically it is difficult to evaluate PC in thicker concrete than 200 mm. We have developed portable 950 keV/3.95 MeV electron linac (linear accelerator)-based X-ray / neutron sources and applied them to inspection of PC concrete thicker than 200 mm within reasonable measuring time of seconds – minutes more than 10 times so far [1–4]. Major poor-construction and degradation of PC bridges to be detected by X-rays and neutrons are unfilled grout,

rainwater intrusion, corrosion and thinning and disconnection of PC wires. Unfilled grout and thinning and disconnection of PC wires can be measured by difference of X-ray attenuation coefficient by X-rays. The three types of the PC bridges and locations of X-ray/neutron source and detector are depicted in **Figure 1**. As for highway bridges, concrete vertical WEB wall is thick as 450–1,000 mm.

There are of course many nondestructive evaluation (NDE) methods to try to detect poor construction such unfilled grout in PC sheath and degradation such as thinning and disconnection of PC wires. RADAR, ultrasonic testing, magnetic testing, 200–400 kV X-ray tube, etc. are candidates as shown in **Figure 2**. However, they are available for thinner concrete than 200 mm. On the other hand, 950 keV / 3.95 MeV X-ray sources can be used for transmission testing for thick concrete of 200–400 mm and 200–1,000 mm based on the calculation and our experience so far [1–4]. We think that only the 950 keV/3.95 MeV X-ray sources can enable transmission imaging of PC structures in 200–1,000 mm thick concrete within minutes.

Figure 3 summarizes major poor construction of unfilled grout, early degradation such as rainwater intrusion and finally serious degradation of thinning and disconnection, and suitable NDE methods and successive structural analysis. If there is unfilled grout in PC sheath, rainwater may intrude from the edges and is stored there. Then, the rainwater makes PC wires and sheath wall be corroded. Volume expansion of PC sheath due to corrosion and oxidation induces cracks in near concrete. The cracks gradually become larger and reach the concrete surface, When the sheath wall is broken, the rainwater exude out and intrude into concrete and surface. As the corrosion is enhanced, superficial oxidized iron leaves and thinning of PC wires occurs. Even, the disconnection may happen since the wires are tensile. Among the above temporal change of state, the structural changes such as unfilled grout and thinning/disconnection of wires can been detected by X-ray transmission imaging. On the other hand, material property change such as rainwater intrusion can be detected by neutron scattering in water. Since concrete vertical WEB wall is thicker than ~450 mm, 3.95 MeV X-ray source is appropriate with respect to transmission ability. Iron components of PC such as wires can be clearly seen with good contrast to concrete. Their thinning and disconnection are observed with the spatial resolution of 1 mm. Since tension is added to PC wires at its construction, they tend to be attached to the upper wall of PC sheath. Therefore, unfilled grout should be recognized under PC wires with certain change of contrast. Measured flaws such as unfilled grout and thinning/disconnection are inputted to structural analysis described in Chapter 5. Thus, initial poor construction of unfilled grout and serious thinning and disconnection of PC wires are diagnosed and then their affect to

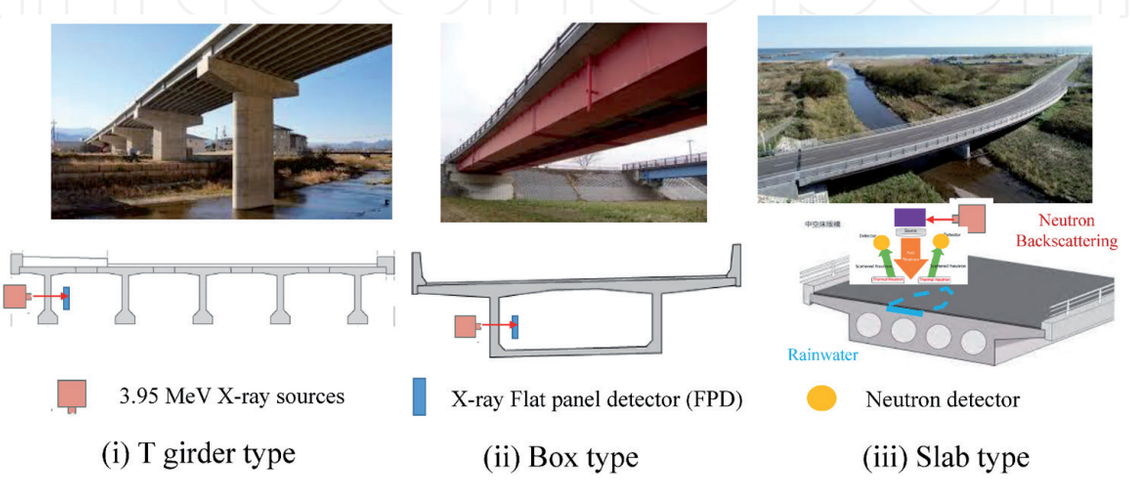

Figure 1.
On-site X-ray/neutron inspection by 3.95 MeV system for three types of highway PC bridge.

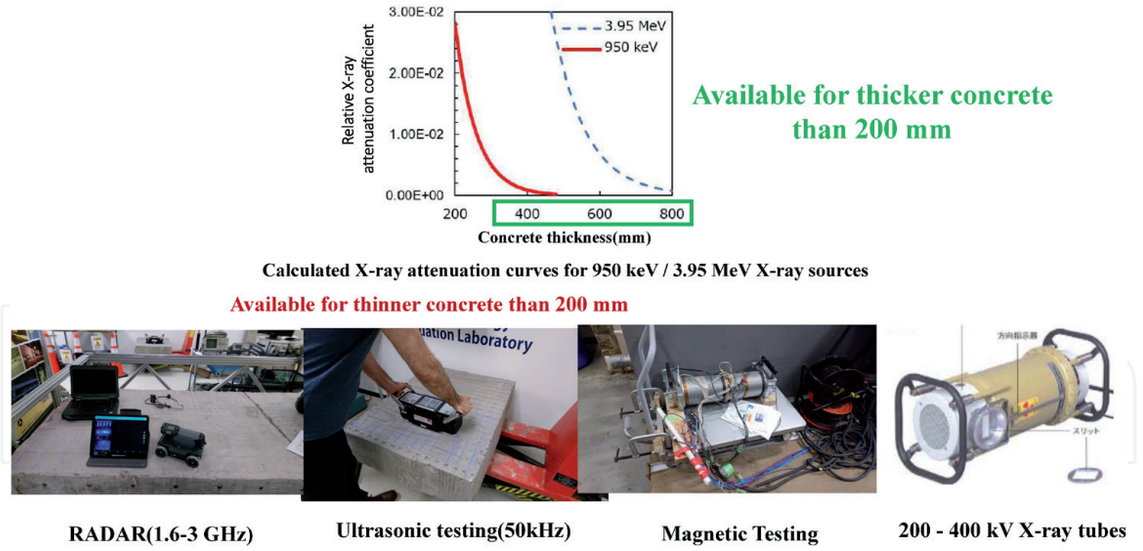

Figure 2.
Advantage of 950 keV/3.95 MeV X-ray sources over other NDE methods for thicker concrete than 200 mm.

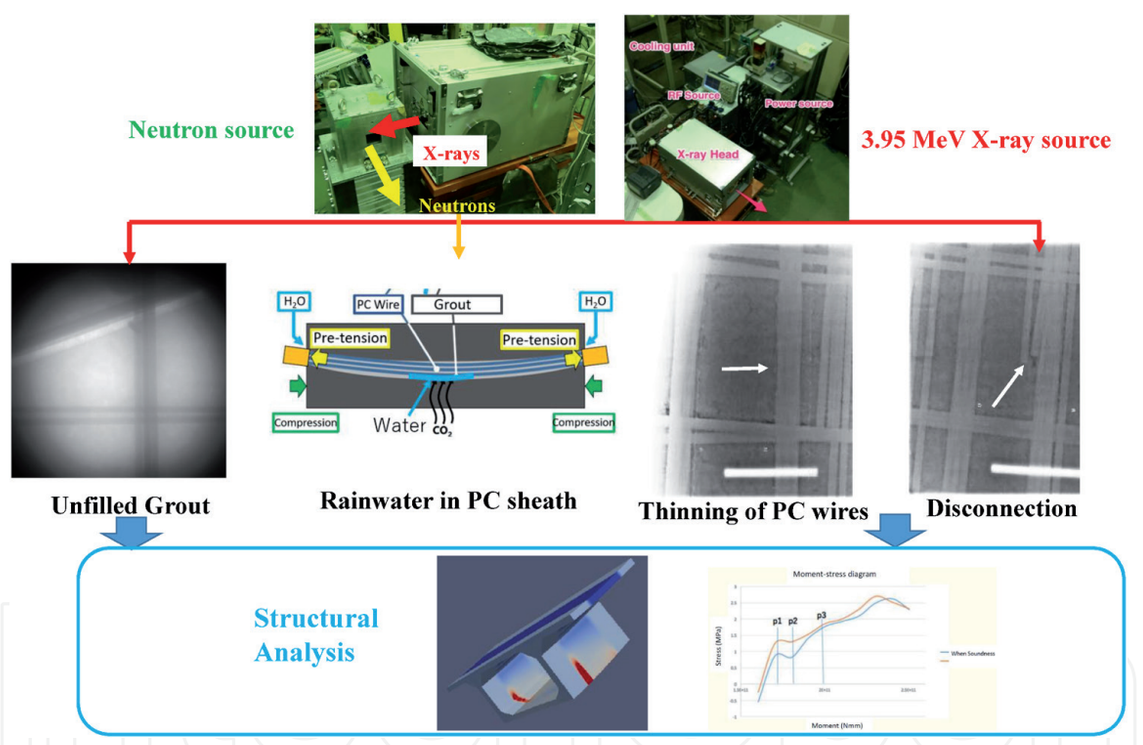

Figure 3.
Poor construction and degradation of PC bridges, suitable NDE methods and structural analysis.

lack and degradation of strength is quantitatively evaluated by structural analysis. Finally, maintenance, repairing and reconstruction are planned. Moreover, there is a possibility to detect rainwater intrusion inside PC sheath by portable 3.95 MeV neutron source [5], which is discussed in Section 3.2.

2. 3.95 MeV electron X-ray/neutron sources

We use X-band (9.3 GHz) linac based 3.95 MeV X-ray sources for the inspection of the actual bridge [1–3]. The systems are shown in **Figure 4**. The electrons are accelerated up to 3.95 MeV by radio frequency (RF) fields. We also adopted the side-coupled standing wave type accelerating structure. Electrons are injected into

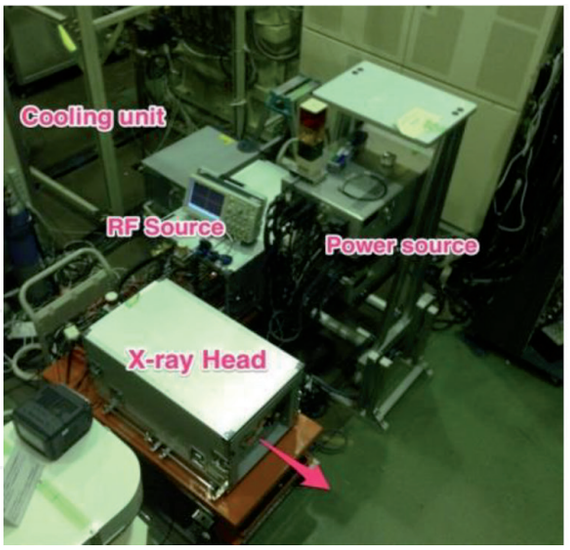

Specification	
RF frequency	9.3 GHz
Beam focusing	RF focusing
X-ray Intensity	2 Gy/min at 1 m
RF source	9.3 GHz Magnetron 1.3MW, Pulse width 4μs Repetition rate 200 pps
Electron gun	Voltage 35kV Pulse Peak Current 300 mA
X-ray head weight	200 kg (with Pd shielding)
RF unit weight	100 kg
Power source	120 kg
Water chiller unit	100 kg

Figure 4.
3 95 MeV portable X-band linac based X-ray source and its major parameters. The system consists of four units: X-ray head, magnetron, power, and chiller units.

a Tungsten target that generates bremsstrahlung X-rays. The generated X-rays are collimated by a Tungsten collimator into the shape of a cone which has an opening angle of 17 degrees. Most important is the X-ray intensity, which is 2 Gy/min at 1 m for a full magnetron RF power of 1.8 MW. The system consists of a 200 kg (including local Pb radiation shielding) X-ray head, 100 kg magnetron box, and stationary electric power source and water chiller unit. The X-ray head and magnetron box are portable, and because they are connected to each other by a flexible waveguide, only the position and angle of the X-ray head are finely tuned. We have optimized the design with respect to X-ray intensity, compactness, and weight. The parameters of the 3.95 MeV X-ray source are summarized in the table in the figure.

We place an X-ray detector on the opposite site of the X-ray source between the object and source to detect the transmitted X-rays through the object. We use a flat panel detector (FPD) by Varian Co. for the detector. The detect and its specification are given in **Figure 5.**

In order to be able to perform neutron TOF measurement, a pulsed neutron source is needed. Usually this kind of neutron source were produced by large-sized, high-energy particle linear accelerator, but by using X-Band type electron linac which compensate its small size with high frequency, the size of the neutron source can be reduced greatly and even possible for mobility.

	XRD 1622 AO19 IMG
Detector Size	16" × 16" (41cm × 41cm)
Energy Range	20keV-15MeV
Scintillator Type	Gd_2O_2S:Tb & Cu Filter PI-200 (Mitsubishi Chemical)
Resolution	200μm Pixel Size
Phosphor Layer	436μm, 200mg/cm²
Frame Rate	1 fps
Electronics	14bit ADC & 2Gain Settings
Interface	Gigabit Ether Net (GigE)
Weight	8.8kg

Figure 5.
X-ray flat panel detector (FPD) and its specification.

When we put a Beryllium target in from of the 3.95 MeV X-ray source, it becomes a neutron source, too (see **Figure 6**). ^{9}Be, having the lowest threshold energy for photo-nuclear reaction ^{9}Be(γ, n)^{8}Be to generate neutrons. A beryllium photo-neutron target (50 mm × 50 mm × 50 mm) has been combined with a lead beam collimator, a boric acid resin layer for neutron shielding, and a lead layer for X-ray shielding. Since mainly fast neutrons are used in the neutron source, a beam line using a high Z material that does not moderate the neutrons is used. Optimization of the beryllium target size and neutron/X -ray shielding simulation is performed using the Monte-Carlo code. The target weight is about 100 kg.

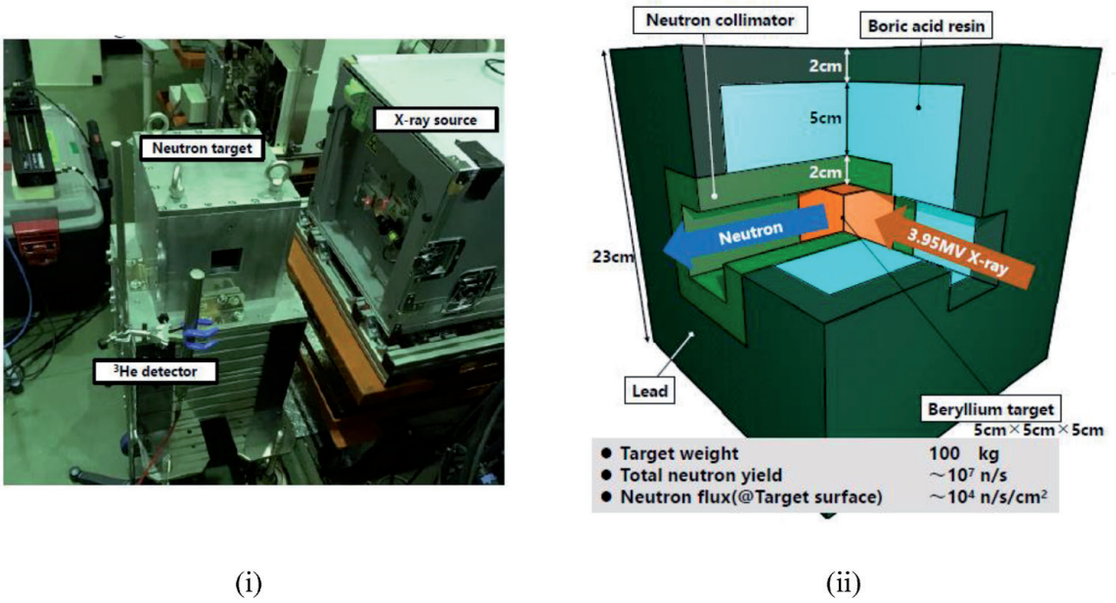

Figure 6.
Neutron source by neutron target in front of 3.95 MeV X-ray source. (i) Photograph (ii) inner structure.

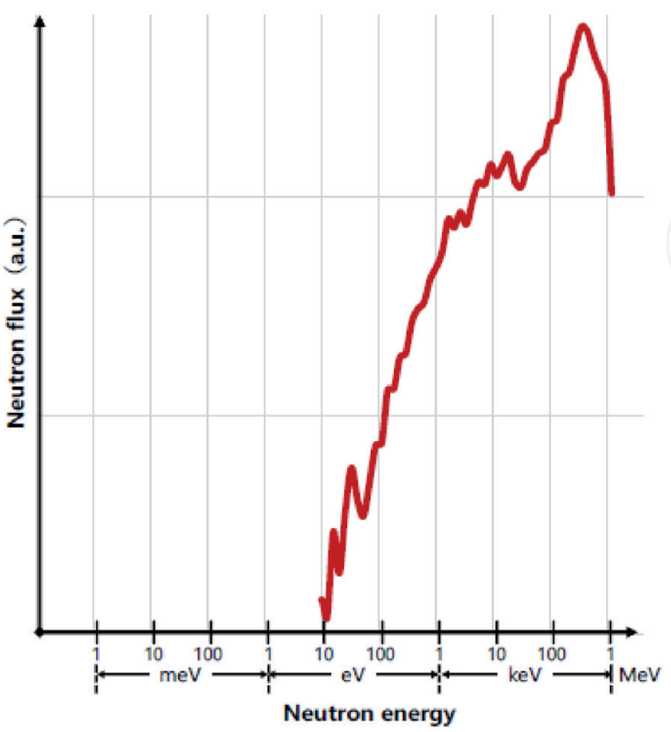

Figure 7.
Produced neutron energy distribution measured by 3He gas detector and TOF method and energy range of neutrons scattered by water.

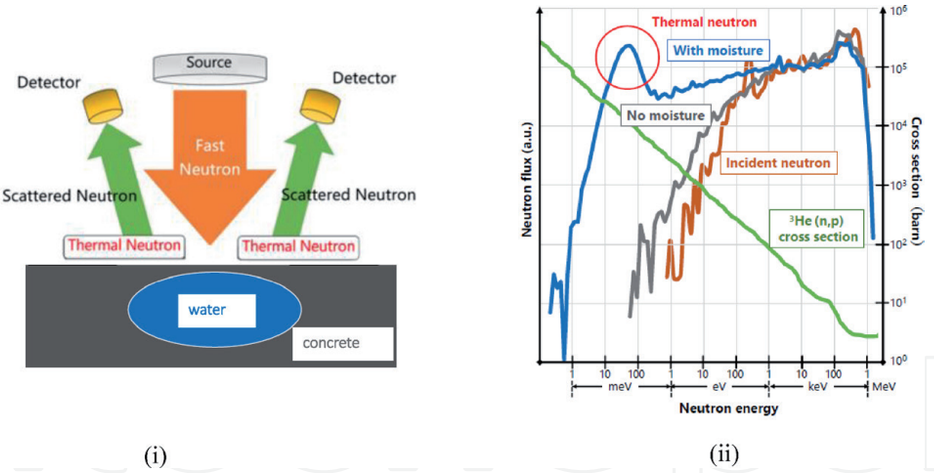

Figure 8.
Neutron energy profiles of ^{3}He gas (n,p) cross section, incident neutrons and backscattered neutrons from concrete with and without water cell. (i) Neutrons scattered by water in concrete. (ii) energies of incident and scattered neutrons in water and ^{3}He gas detector efficiency.

The calculated neutron yield in the neutron source is approximately ~10^{7} n/s (neutrons/second), which is more intense than ~10^{6} n/s of ^{252}Cf (1 μg) moister detector used for NDE in chemical plants. The distribution of neutron energy produced is measured by ^{3}He gas detector and TOF (Time of Flight) method, as shown in **Figure 7**.

Rainwater detection using the 3.95 MeV neutron source is performed by irradiating concrete with fast neutrons and detecting backscattered moderated neutrons due to multiple elastic scattering with light elements especially hydrogen nuclei (see **Figure 8(i)**). Neutron detection using the ^{3}He gas is attributed to high reaction cross section with neutrons in the thermal region. Therefore, the count of detectors increases with the existence of water as shown in the figure.

3. X-ray transmission detection and evaluation for highway bridge by 3.95 MeV X-ray source

We plan to do NDE by 3.95 MeV X-ray source for highway PC bridge in 2020. Its goal is to detect and visualize unfilled grout via X-ray transmission imaging. **Figure 9** shows transvers and longitudinal cross sections, possible location of unfilled grout and typical X-ray transmission images by 950 kV source for filled and unfilled grouts. Since tensile PC wires tends to attach the upper inner surface in PC sheath, the grout is filled in the lower space there. Therefore, in general, unfilled grout occurs in the lower space (see (i), (ii)). In construction stage, grout is pushed and filled from one side of sheaths so that unfilled grout tends to occur at an ascending part of the opposite side as shown in (iii). The unfilled grout in PC sheathe in 200–250 mm thick T girder WEB was measured and visualized at the ascending part as show in (iv). The unfilled part looks white comparing gray or black part of filling. Phase of unfilled can be evaluated by quantitative evaluation of gray value, namely X-ray attenuation coefficient. Appearing X-ray transmission imaging of filled and unfilled grout would be a goal of the coming task for highway PC bridges.

Here we consider PC bridges of box type and T girder Typical cross section, location of PC sheath, X-ray head and detector are summarized in **Figure 10**. X-ray head is movable 200 kg weigh component among the four. It can be accessed to the WEB with RF source via flexible waveguide for RF power delivery for electron beam acceleration. For example, the thickness of WEB of Box type and T girder are

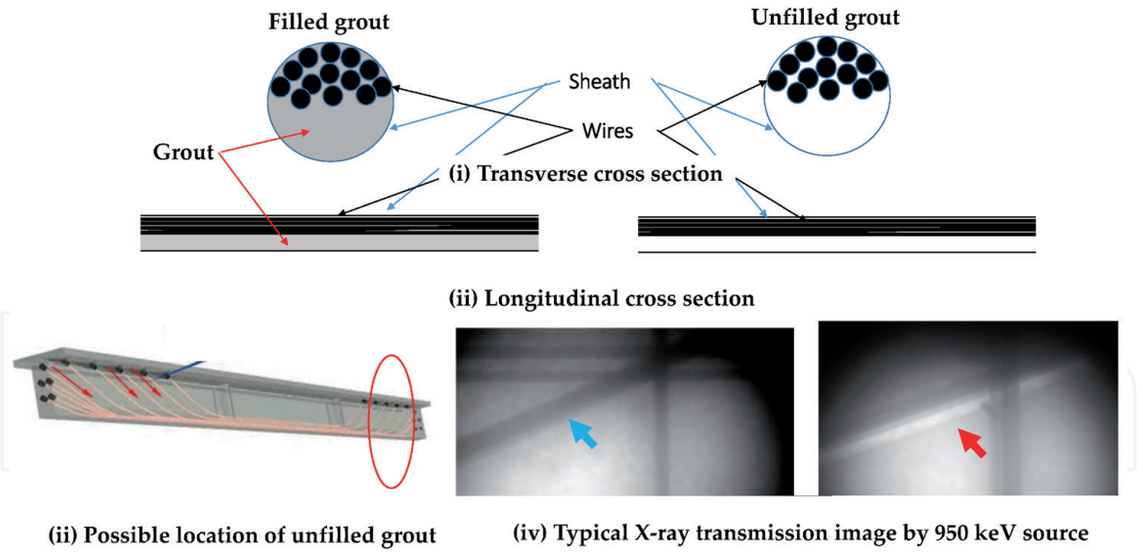

Figure 9.
Transvers and longitudinal cross sections, possible and typical X-ray transmission images by 950 kV source for filled and unfilled grouts.

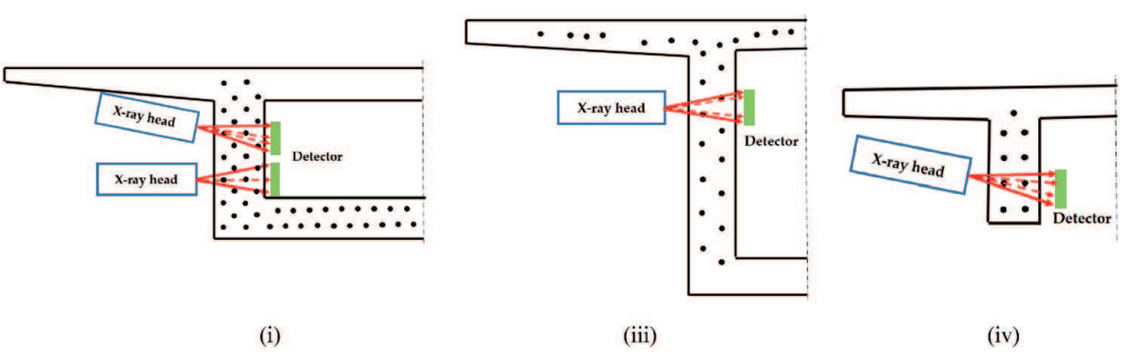

Figure 10.
Typical WEBs and locations of X-ray source and detector for box-type and T. (i) Box thick WEB. (ii) box thin WEB. (iii) T-girder WEB.

750, 550 and 450 mm, respectively. Closed circles represent typical locations of PC sheaths. Vertical arrays of PC sheaths are arranged in the zigzag way ((i), (ii)) and at the same vertical level ((iii)). When we allocate the X-ray head and eject X-rays horizontally, PC sheaths can form separate images at the detector for two zigzag arrays (see (ii)). However, in the lower case of (i) two images of the PC sheaths at the same vertical level are overlapped at the detector. In order to obtain two transmitted images for the above case, we allocate the X-ray head higher by about 100 mm and decline it by about 10 degrees as shown in the upper case of (i) and (iii). WE have almost finalized the way of access and allocation of the X-ray head to all cases as shown in the figure.

We have carried out the simulating experiments for real highway bridges inspection in the configuration of **Figure 10(i)–(iii)**. In order to simulate the concrete thickness and number and location of PC sheaths, we use cut samples from real old PC bridges which were deconstructed after finishing their roles as shown in **Figure 11(i)**.

First, we explain the results of separate X-ray transmission images for two PC sheaths at different vertical level as shown in **Figure 11(ii)**. Total concrete thickness is 750 mm and 10 iron PC wires of 70m$^{\phi}$ are inserted to vacant Sheath 1 and 2. X-ray shot duration is 10 s and it is summed by 100 times. Original image is (ii) and (iii) is the boundary enhanced image by the principle of local contrast enhancement using gray level of the neighborhood pixels [6]. The two PC sheaths and wires are clearly

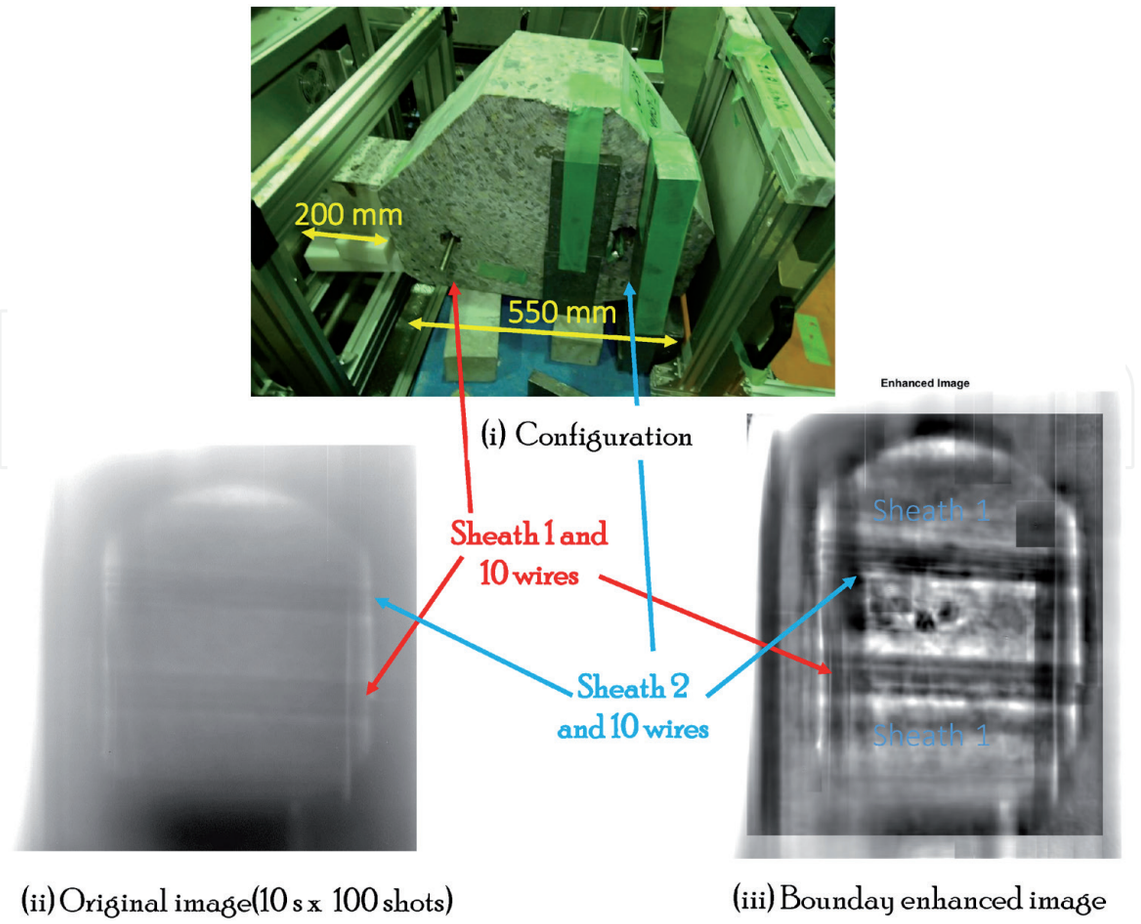

Figure 11.
Separate X-ray transmission images for two PC sheaths at different vertical level.

recognized separately in both images. In the boundary enhanced image, the sheath and unfilled grout looks clearer than the original, although its background becomes noisy. Instead, the original image is totally ambiguous, but the sheaths wires can be recognized.

Second, we measured three PC sheaths at the same vertical level and horizontal X-ray ejection as shown in **Figure 12**. From the left X-ray source as (i), (ii), 10 wires are inserted in the lower space of the first PC sheath 1. Grout remains in the half space of the second PC sheath 2. The third PC sheath is vacant. X-ray transmission images were obtained by 10 s duration times 1 and 100 as shown in (iii), (iv), respectively. There is almost no remarkable difference as to the quality of image. Only wires in the lower space and upper vacant space, which corresponds to unfilled grout, in the PC sheath 1 can be seen and the PC sheaths 2, 3 are hidden behind it. Since PC wires are attached to the upper inner surface of sheath in a real case, real image is upside down of these images.

Third, the configuration and transmission images for three same vertical level PC sheaths and 100 mm up −10 degree declining X-ray ejection are given in **Figure 13**. Here we try to get separate images for the three same vertical level PC sheaths at the detector. Images by 10 s duration times 1 and 100 shots are shown in (ii) and (iii), respectively. Again there is no remarkable difference with respective to image quality between them. Here the three PC sheaths are becoming separate, but still partially overlapped. We can surely recognize that PC wires are inserted from the right hand side and stop in front of the left edge in the nearest PC sheath 1 to the X-ray source. Over the PC sheath 1, we can see the PC sheath 2 with partially filled grout. The oblique edge of grout is seen in the left hand side. Finally, vacant PC sheath 3 is observed over the PC sheath 2.

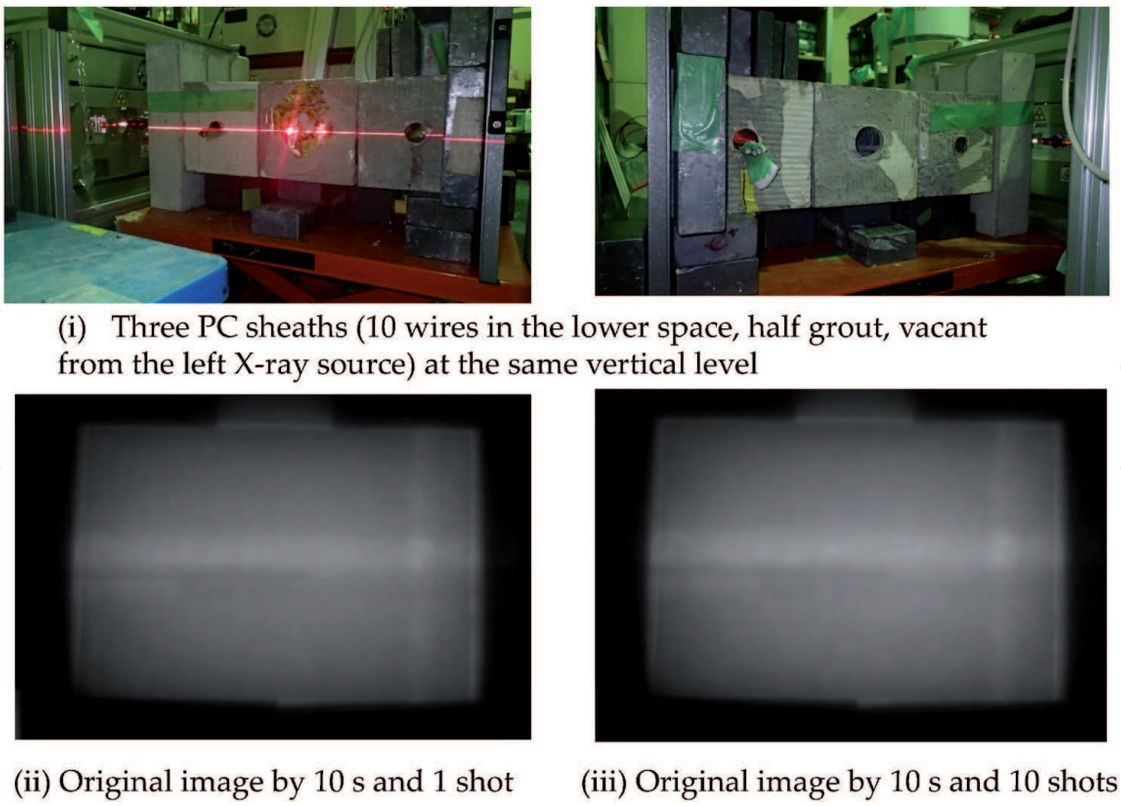

Figure 12.
Image of three PC sheath at the same vertical level and X-ray horizontal ejection.

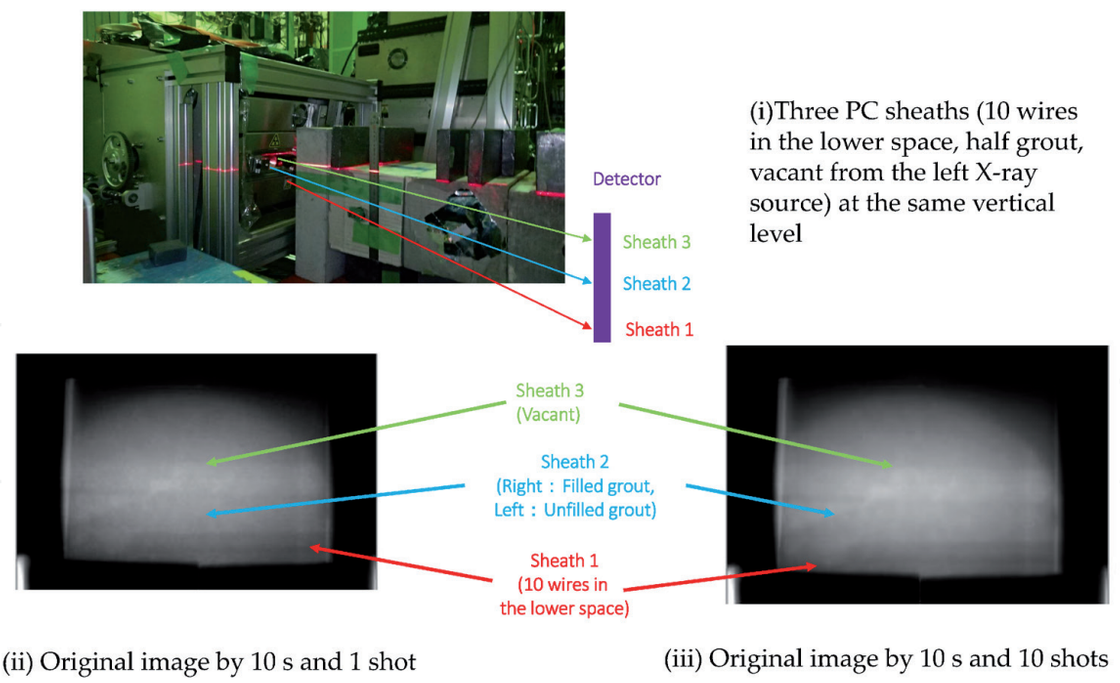

Figure 13.
Configuration and transmission images of three PC sheaths at the same vertical level and 100 mm level up and – 10 degree declining ejection of X-ray source.

Now the findings are summarized in the following.

- Transmission image of 750 mm thick concrete is completely obtained in 10 s by 3.95 MeV X-ray source. We should understand this fact comparing to the calculated X-ray attenuation in the upper graph of **Figure 2**.

- In any cases, PC iron wires can be easily found due to their rather black images. Then, the existence and location of PC sheath is detected. Furthermore, thinning and disconnection can be analyzed.

- In case of several same vertical level PC sheaths and horizontal X-ray ejection, only nearest PC sheath is clearly seen and others are hidden behind it.

- In case of several same vertical level PC sheaths and upward shifted and declining X-ray ejection, they form separate images. Thus, we can detect and evaluate the far side PC sheath.

- Unfilled grout can be evaluated by gray value with respect to rather black image of PC wires in positive image processing. We may be able to form a correlation between measured relative gray value and stage of unfilled grout.

4. Rainwater detection in PC sheath by 3.95 MeV neutron source

Now we are going to explain detection of rainwater intrusion by neutrons. Images of rainwater intrusion in PC bridge and slab type bridge are depicted in **Figure 14**. Rainwater intrusion at unfilled grout in PC sheath causes corrosion of wires to thinning and disconnection, and finally degradation of strength of bridge. We try to detect them by the 3.95 MeV neutron source and ^{3}He gas detector via neutron backscattering. It is expected to be monitoring of early degradation of bridge strength before corrosion of PC wires.

Here we have just started basic experiment on water detection by neutron backscattering considering the situations depicted in **Figure 14**. **Figure 15** shows the experimental configuration. We just put a 50 mm thick bottle of water on a T girder concrete sample cut from a real old bridge. Neutrons from the 3.95 MeV source are scattered in water in the bottle. Backscattered neutrons are detected by the ^{3}He detector, and the TOF method is applied to measure the time of flight from the scattering point to the detector. Flight distance divided by the measured time becomes the velocity of neutron, v and its kinetic energy is obtained as, $\frac{1}{2}mv^2$, for nonrelativistic case.

Measured results of neutron counts as a function of TOF and converted energy are given in **Figures 16(i)** and **(ii)**, respectively. Neutron counts as a function of measurement time and converted neutron energy in cases of unfilled and filled water are plotted in (i) and (ii), respectively. Since the neutron source with about 10^7 n/s is not necessarily intense, the difference with/without water is not remarkable. But we can clearly observe component of neutron backscattering below 1 eV as predicted in **Figure 8**. It can be understood that Proof-of-Principle has been verified.

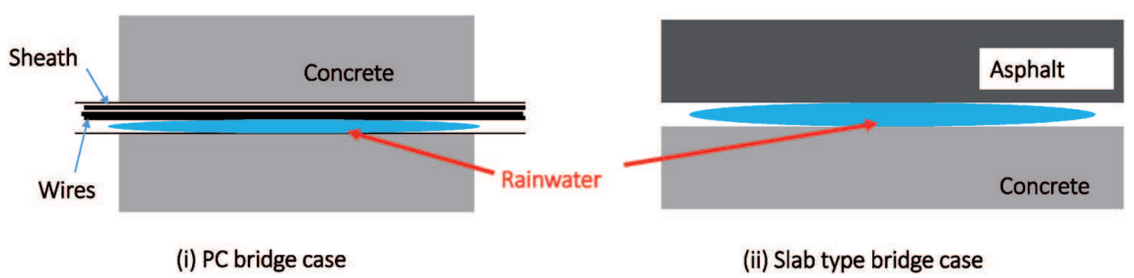

Figure 14.
Images of rainwater intrusion in PC bridge and slab type bridge.

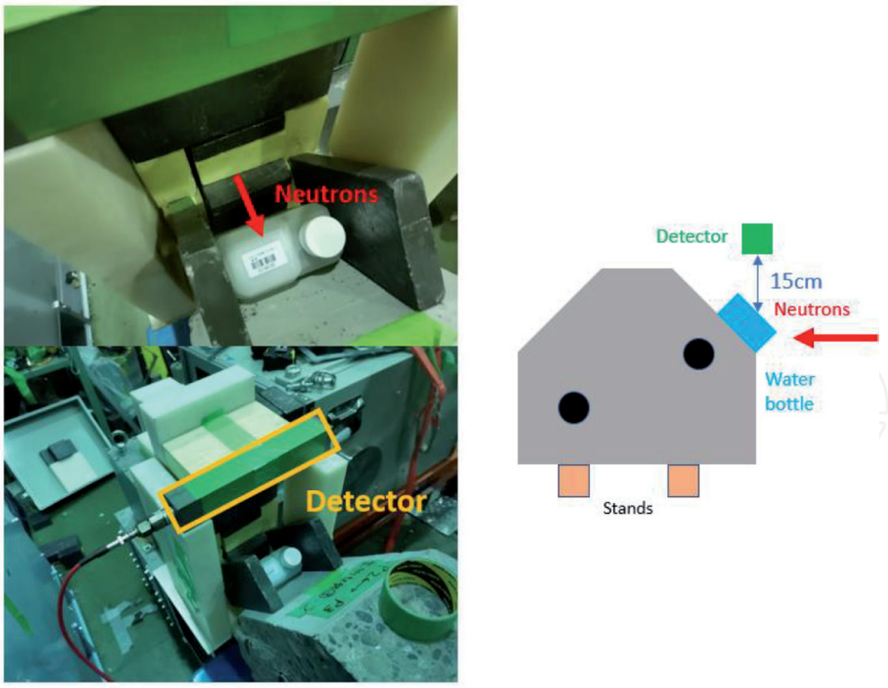

Figure 15.
Experimental configuration modeling rainwater detection by neutron scattering.

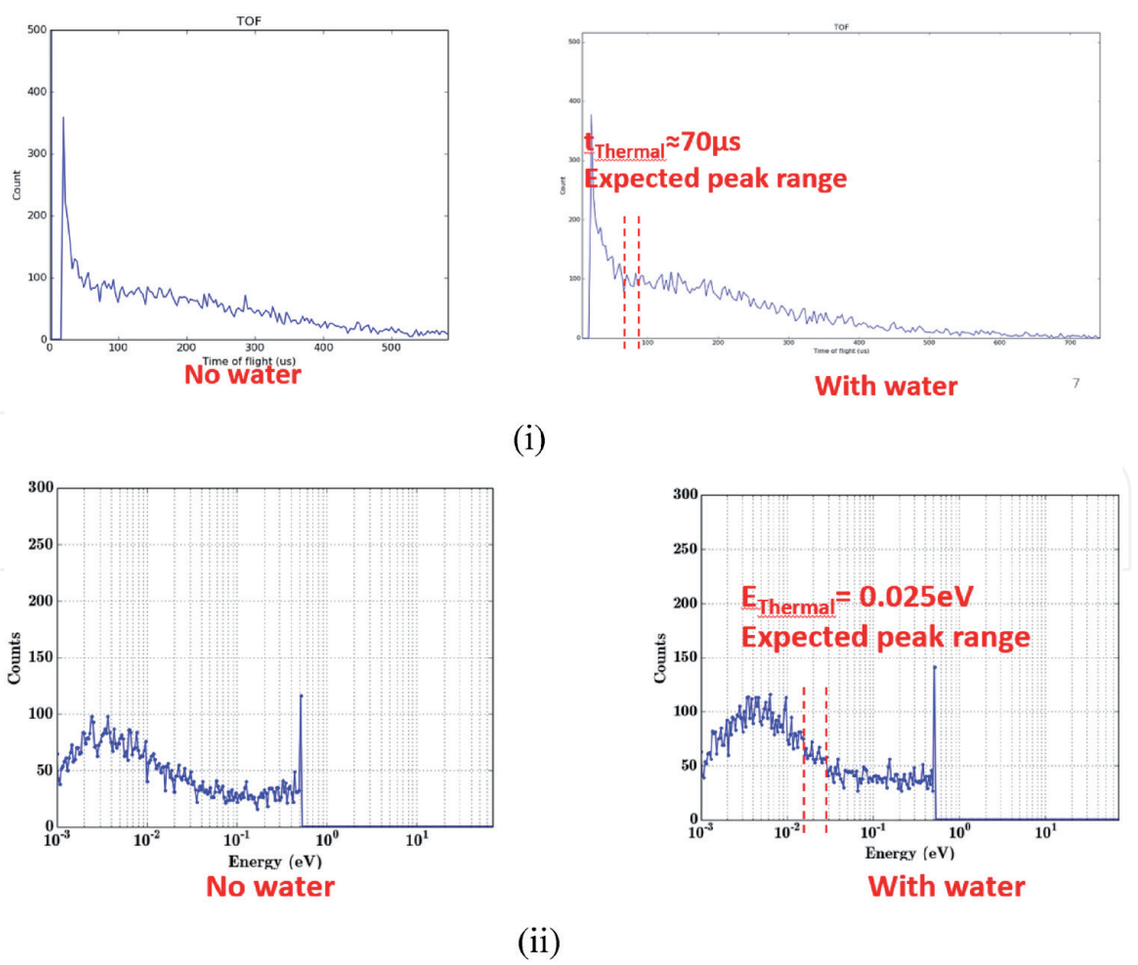

Figure 16.
Comparison of measured backscattered neutron count as a function of TOF with and without water. (i) Neutron counts as a function of TOF. (ii) neutron energy spectra.

As a next step, we are to perform numerical analysis using Monte Carlo code considering the case to detect rainwater in the configuration for slab bridge type. Multilayer sample with asphalt (~75 mm thick), water (more than few mm thick) and concrete (very thick) is first adopted.

5. 3D structural analysis using finite element method

In order to accurately reflect the influence of more detailed degradation conditions obtained by X-ray imaging on structural performance, three-dimensional finite element analysis is required. This chapter aims to evaluate structural strength degradation more precisely by performing structural calculation using finite element analysis software, Du COM-COM3 [7], that can simulate the nonlinear behavior peculiar to concrete with high accuracy. Effect of degradation is evaluated through stress distribution in the cross section of the bridge obtained by the analysis.

The software used for the analysis is DuCOM-COM3 which continues to be developed by the Concrete Laboratory, Department of Civil Engineering, Faculty of Engineering, University of Tokyo [7]. DuCOM-COM3 is used to calculate the mechanical behavior of structures with multi-spans from dynamic characteristics such as earthquake motion and wind vibration to long-term deformation behavior over several decades. DuCOM, which is responsible for the calculation of movement and material deterioration, is coupled to construct structures at various scales from the molecular-scale microscale to the structure-level macroscale.

We introduce an example to use DuCOM-COM3 for evaluation of strength degradation due to measured PC flaws. **Figure 17** shows X-ray transmission images of thinning and disconnection of PC wires of a box type bridge and evaluation of cross section reduction. Degradation of this bridge due to salty water used in winter is rather serious. At the most serious cross section, several PC sheaths are broken and PC wires are heavily thinned and disconnected. We try to evaluate reduction of PC wire cross section as shown in the table of the figure. Then, we input the data to DuCOM-COM3 analysis. **Figure 17** shows one example of box type bridge.

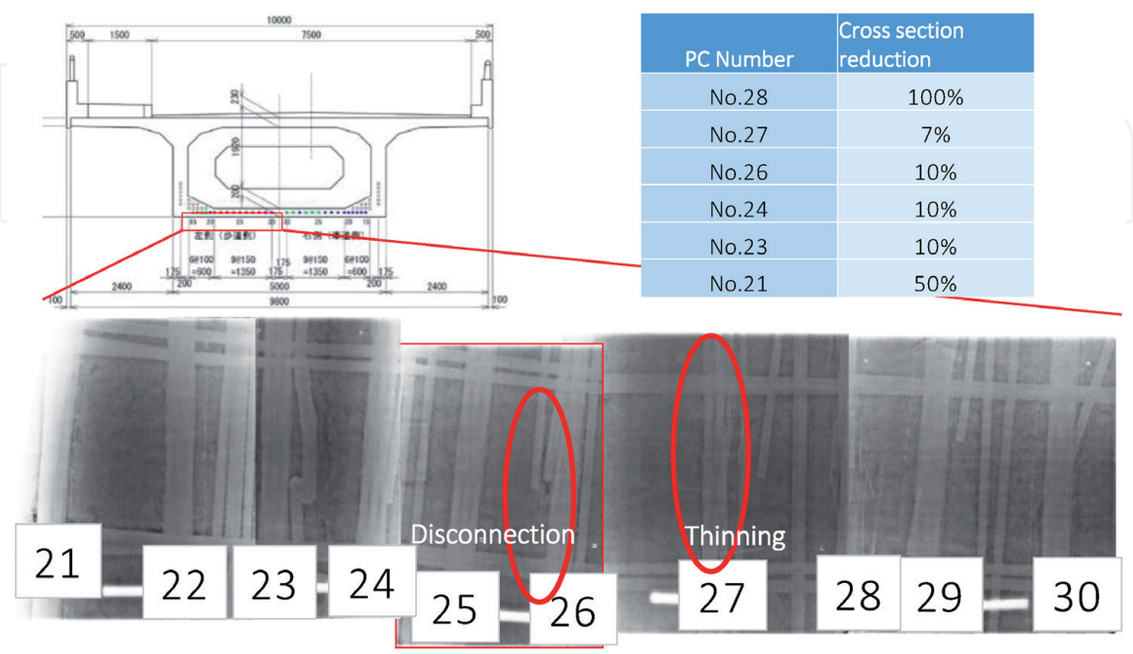

Figure 17.
X-ray transmission images of thinning and disconnection of PC wires of a box type bridge and evaluation of cross section reduction.

We consider a partial block of one span of a four-span PC bridge (see **Figure 17**). We measured most degraded floor cross section by using our X-ray source. Several X-ray transmission images were obtained as shown in the figure. Due to long term corrosion due to salty water, several PC sheaths are broken and some PC wires are thinned and disconnected. Reduction of PC wires cross section is approximately evaluated as shown in the figure. Those data are used for the structural analysis.

3D mesh model is depicted in **Figure 18**. The whole mesh structure corresponds to a part of one span of a four span box type PC bridge. We adopt specialized boundary condition and standard vertical load. Then, we calculate 3D distribution of bending moment, stress, strain and displacement.

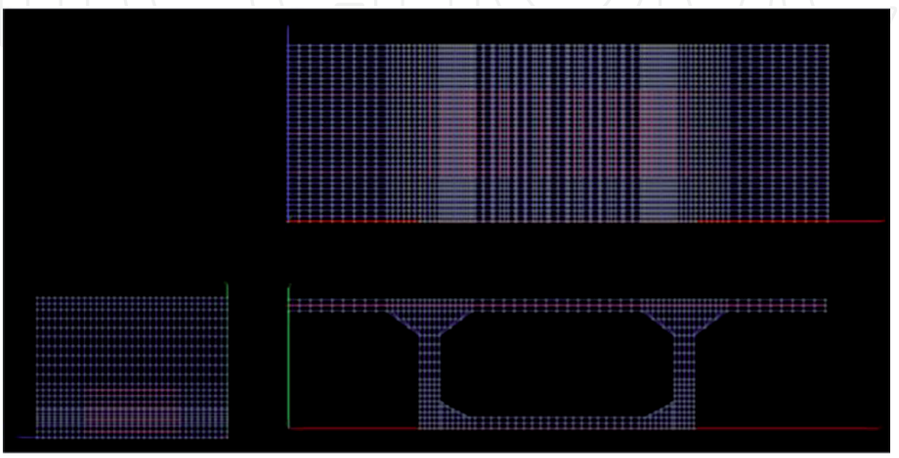

Figure 18.
3D mesh model for the box type bridge with cross section reduction of PC wires at a certain cross section of the bridge.

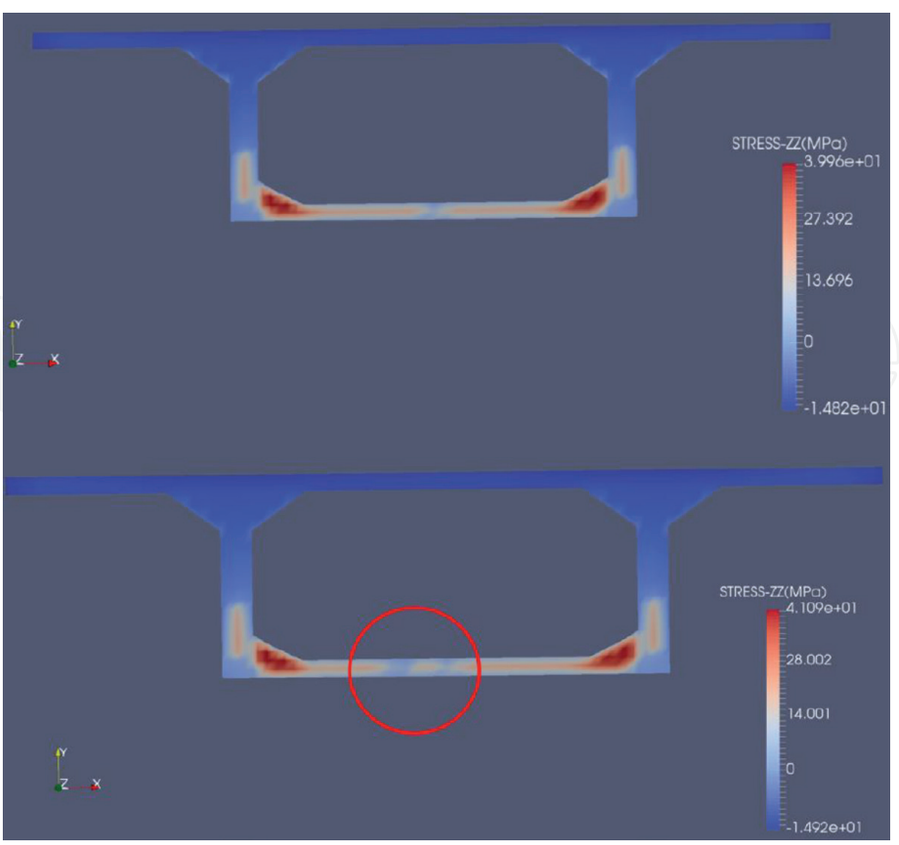

Figure 19.
Comparison of 3D stress distribution of initial (healthy) and degraded states. Circle indicates the degraded part.

3D stress distribution of initial (healthy) and degraded states are given in the upper and lower images of **Figure 19**, respectively We can observe discontinuous distribution around the degraded part indicated by the circle. **Figure 20** also shows the fracture points confirmed by the overall 3D model in this model and analysis.

Figures 21 and **22** show the moment-stress distribution and moment-strain distribution at the lower edge of the bridge section for the initial and degraded states. In both cases, the horizontal axis is the moment, and the vertical axis is the stress and strain. If we can eliminate the moment, we can get standard stress – strain relation. Anyway, we can clearly observe yield phenomenon and yield stress. The upper and lower curves represent the results for the initial and degraded states. Reduction of yield stress is clearly seen due to the degradation. The reduction is 5% in this case. This reduction would be rather serious for the maintenance of the bridge. Actually, it has been decided that this bridge should be reconstructed.

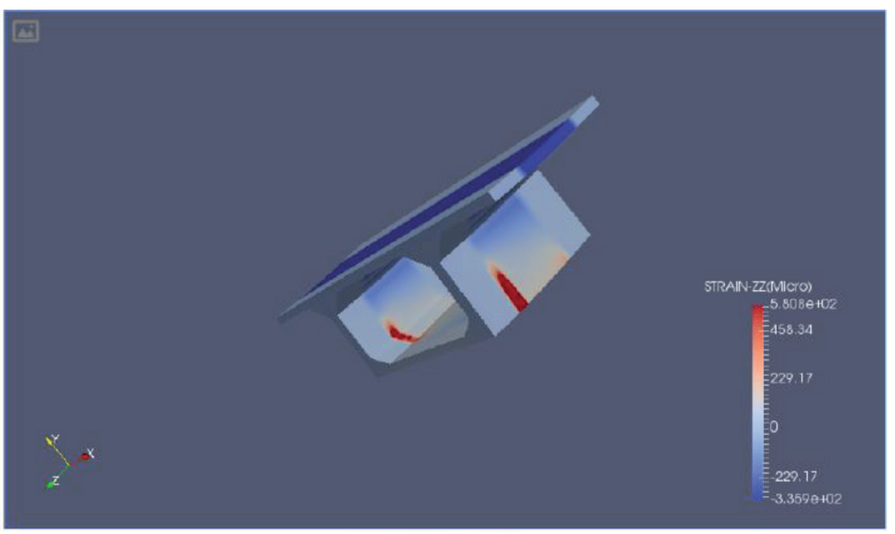

Figure 20.
Confirmation of fracture site in the 3D model.

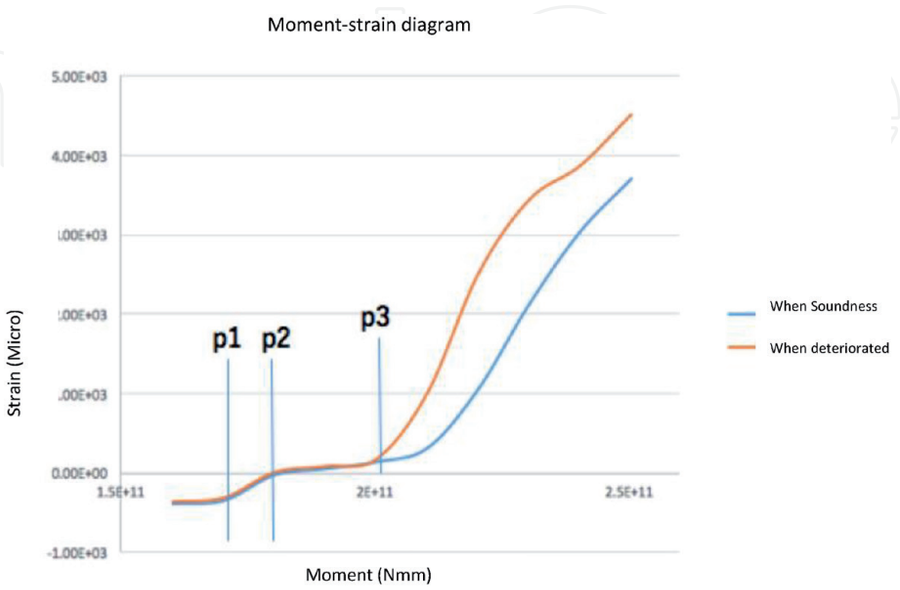

Figure 21.
Moment-stress graph at bottom edge of bridge section.

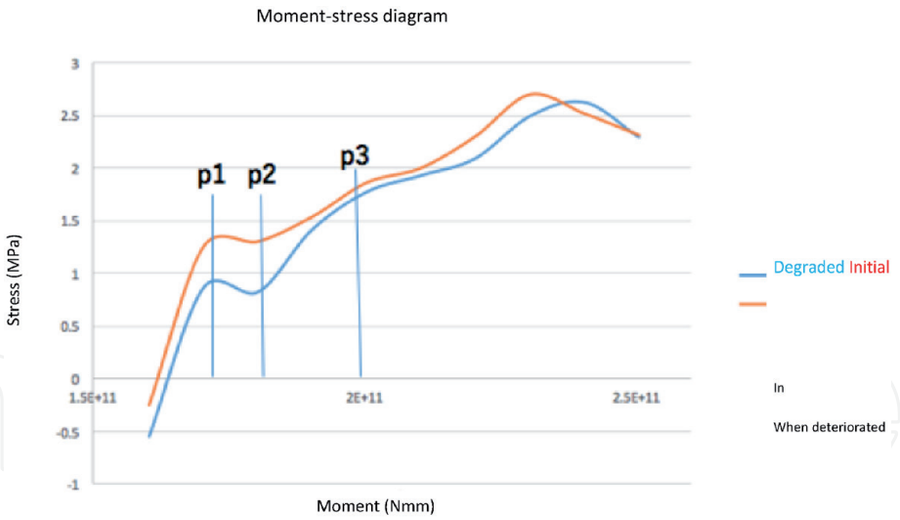

Figure 22.
Moment-strain graph at bottom edge of bridge section.

6. Guidelines for special inspections using 950 keV/3.95 MeV X-ray sources

The Public Works Research Institute and the University of Tokyo are developing new technical guidelines for special inspections of bridges using 950 keV/3.95 MeV X-ray sources. An overview is provided in **Figure 23** [4]. First, visual and hammer sound inspection screening should be performed based on regular inspection guidelines. Advanced hardware and software techniques such as drawn and acoustic analysis are adopted in this step. If degraded parts are found, the special X-ray transmission inspection is performed using the 950 keV or 3.95 MeV X-ray sources, depending on the thickness of the concrete containing the degraded parts (see **Figure 2**). Here, the states of PC wires such as unfilled grout and thinning/disconnection are quantitatively evaluated with spatial resolution of 1 mm. Especially, the state of unfilled grout can be evaluated quantitatively by measuring

Figure 23.
Guidelines for special X-ray transmission inspection using 950 keV/3.95 MeV X-ray sources accompanied with visual and hammering-sound inspections, structural analysis, final repair, and/or reinforcement.

the gray value, namely the X-ray attenuation coefficient, under the criterion from 0 (white: vacant) through 1 (black as PC wire) (see **Figure 24**). NDE of unfilled grout by γ-emitter radioisotope using such a phase control and decision to proceed to destructive evaluation to obtain more precise information are under way by IFSTTAR (French Institute of Science and Technology for Transport Development and Networks) in France [8]. Then, we plan to perform 3D structural analysis to evaluate the degradation of the structural strength quantitatively as shown in **Figure 25**. We have introduced one example of the structural analysis and evaluation of reduction of yield stress due to thinning and disconnection of PC wires by using DuCOM-COM3 in Chapter 5. We propose regular X-ray transmission inspection and structural analysis every five years and record the change of yield stress. In order to confirm validity of numerical results, we plan to use not only DuCOM-COM3 code but also ATENA code [9]. The results by the two codes are compared and checked. If we observe remarkable change in both results, we may proceed to more careful consideration. Based on this evaluation, repair, reinforcement, or other decisions should be taken into account. We are going to start practical

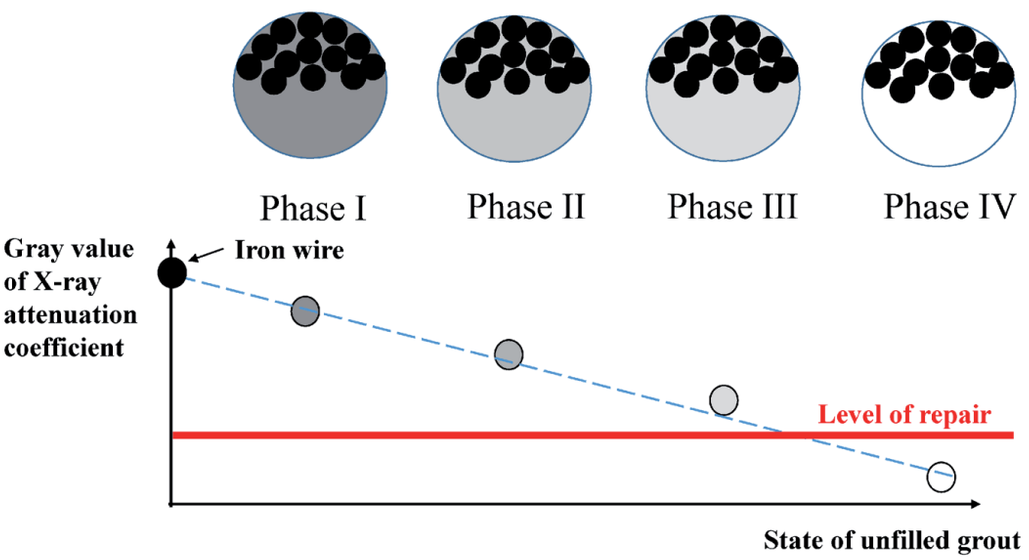

Figure 24.
Phases of unfilled grout and relation with gray value of X-ray attenuation coefficient.

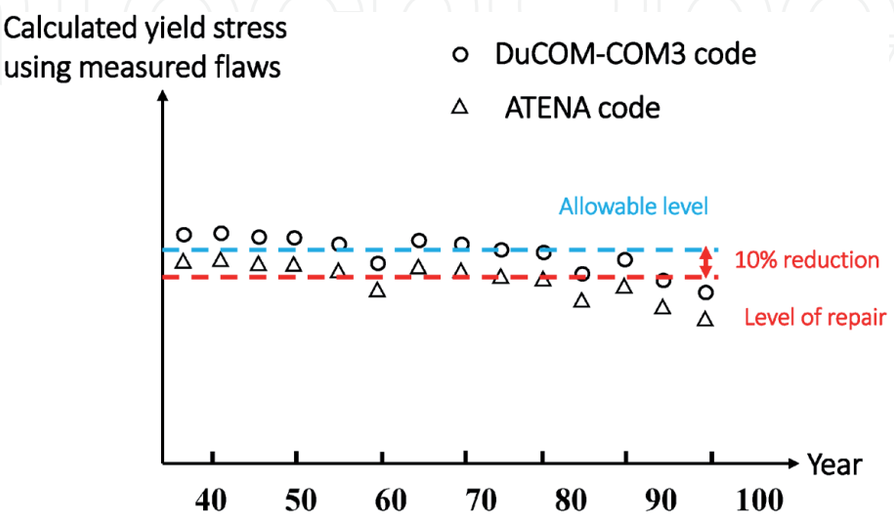

Figure 25.
Proposal of quantitative criterion for regular X-ray inspection and structural analysis with respective to measured property of mechanical strength.

and commercial highway bridge X-ray inspection under collaboration with major industries. We hope to apply these guidelines to all aged bridges in Japan and finally across the world in near future.

7. Conclusion

We are going to apply our 3.95 MeV X-ray source to highway PC bridge inspection in Japan in 2020. Among T-girder-, box- and slab-type bridges, we first inspect box type bridge with 550–750 mm thick WEB wall. We use 950 keV/3.95 MeV x-ray sources for thinner than 300 mm and 300–1,000 mm WEB walls, respectively. Main purpose is to visualize and evaluate unfilled grout in PC sheath. We performed preliminary experiments considering real situations to obtain X-ray transmission images of wires and unfilled grout of several PC sheaths. We successfully obtain one X-ray transmission image within 10 s. We also adopt boundary enhancement image processing to check the state of PC sheath, wires and grout. We also succeeded in obtain separate images of same vertical level PC sheaths by changing vertical location and angle of the X-ray source. In all cases, PC wires can been easily seen by black images and then we can recognize the location of PC sheath. Next, we check unfilled grout beneath the wires. We propose to use the gray value, namely relative X-ray attenuation coefficient, to evaluate of the state of unfilled grout.

Moreover, we try to apply 3.95 MeV neutron source in order to detect rainwater between surface asphalt and concrete. We successfully detected the existence of water via neutron back scattering in water. As a next step, we try to verify the rainwater detection in slab type bridge.

We also performed 3D structural analysis for box type bridge by using DuCOM-COM3 code. 5% reduction of yield stress due to thinning and disconnection PC wires via rainwater corrosion was evaluated. From now on, we are going to analyze mechanical strength reduction due to unfilled grout.

Finally, we propose a guideline for regular maintenance control by making use of 950 keV/3.95 MeV X-ray sources and structural analysis codes of DuCOM-COM3 and ATENA. After we verify the inspection of box type bridge in 2020, we plan to inspect other box- and T-girder-bridged in 2021.

Acknowledgements

This work was supported by the "Infrastructure Maintenance, Renovation, and Management program" of Cross-ministerial Strategic Innovation Promotion Program (SIP), Cabinet Office, Government of Japan in 2015-2019. We would like to thank Mr. Yasuhiro Ishida of the Public Works Research Institute of Japan for the total management, Prof. Yasuo Tanaka of Kanazawa Institute for Technology for the structural analysis and Mr. Hiroaki Takeuchi and Mr.Jean-Michel Bereder who are the graduates of Uesaka laboratory of Department of Nuclear Engineering and Management, the University of Tokyo for their related master thesis works.

Author details

Mitsuru Uesaka[1*], Katsuhiro Dobashi[1], Yuki Mitsuya[1], Jian Yang[1] and Joichi Kusano[2]

1 Nuclear Professional School, Institute of Engineering Innovation, The University of Tokyo, Ibaraki, Japan

2 Accuthera Inc., Kawasaki, Kanagawa, Japan

*Address all correspondence to: uesaka@tokai.t.u-tokyo.ac.jp

IntechOpen

References

[1] Uesaka M et al. 950 keV, 3.95 MeV and 6 MeV X-band linacs for nondestructive evaluation and medicine. Nucl. Instrum. Methods Phys. Res. A. 2011;657:82-87.

[2] Uesaka M et al. Commissioning of portable 950 keV/3.95 MeV X-band linac X-ray source for on-site transmission testing. J. Adv. Maint. 2013;5:93-100.

[3] Uesaka M et al. On-site Non-destructive Inspection of the Actual Bridge using the 950 keV X-band Electron Linac X-ray Source. J. Disaster Res. 2017;12:578-584.

[4] Mitsuru Uesaka, Yuki Mitsuya, Katsuhiro Dobashi, Joichi Kusano, Eiji Yoshida, Yoshinobu Oshima, Masahiro Ishida, "On-site Bridge Inspection by 950 keV / 3.95 MeV Portable X-band Linac X-ray Sources", Bridge Optimization - Inspection and Condition Monitoring, IntechOpen, 2018, DOI: 10.5772/intechopen.82275

[5] Bereder J M. et al. Development of 3.95 MeV X-band linac-driven x-ray combined neutron source. Journal of Physics: Conference Series 874 (2017) (1) 012104. DOI: 10.1088/1742-6596/874/1/012104

[6] Pei C, Wu W, Uesaka M. Image enhancement for on-site X-ray nondestructive inspection of reinforced concrete structures. Journal of X-Ray Science and Technology. 2016;24: 797-805. DOI: 10.3233/XST, 160588s

[7] K. Maekawa, A. Pimanmas and H. Okamura: Nonlinear mechanics of reinforced concrete, Spon press, London, 2003.

[8] Robert GUINEZ Chef de l'unite technique Radiographie, Radioscopie Laboratoire Regional des Ponts et Chaussees de Blois and Eric HOYRUP, Directeur du Laboratoire Regional des Ponts et Chaussees de Blois Chef de l'agence Centre du CETE Normandie-Centre, Controle non destructive des ouvrages d'art par gammagraphie, radiographie et radioscopie, Bull. liaison Labo. P. et Ch. -171 -janv.-fevr. 1991 -Ref. 3550.

[9] Tereza Sajdlová, ATENA Program Documentation Part 4-8, ATENA Science – GiD Construction Process Tutorial, https://www.cervenka.cz/assets/files/atena-pdf/ATENA.